Echo-planar MR imaging of dissolved hyperpolarized 129Xe.

Månsson, S.; Johansson, Edvin; Svensson, J.; Olsson, L. E.; Ståhlberg, Freddy; Petersson, J. S.; Golman, K.

Published in:
Acta Radiologica

DOI:
10.1034/j.1600-0455.2002.430503.x

2002

Acta Radiologica 43 (2002) 455–460
Printed in Denmark · All rights reserved

ACTA RADIOLOGICA
0284-1851

ECHO-PLANAR MR IMAGING OF DISSOLVED HYPERPOLARIZED ^{129}Xe

Potential for MR angiography

S. Månsson[1], E. Johansson[2], J. Svensson[3], L. E. Olsson[3], F. Ståhlberg[4], J. S. Petersson[5] and K. Golman[5]

[1]Department of Experimental Research, Malmö University Hospital, [2]Department of Radiation Physics, Lund University Hospital, [3]Department of Radiation Physics, Malmö University Hospital, [4]Department of Radiology, Lund University Hospital, and [5]Amersham Health R&D, Medeon, Malmö, Sweden.

Abstract

Purpose: The feasibility of hyperpolarized ^{129}Xe for fast MR angiography (MRA) was evaluated using the echo-planar imaging (EPI) technique.

Material and Methods: Hyperpolarized Xe gas was dissolved in ethanol, a carrier agent with high solubility for Xe (Ostwald solubility coefficient 2.5) and long relaxation times. The dissolved Xe was injected as a bolus into a flow phantom where the mean flow velocity was 15 cm/s. Ultrafast EPI images with 44 ms scan time were acquired of the flowing bolus and the signal-to-noise ratios (SNR) were measured.

Results: The relaxation times of hyperpolarized Xe in ethanol were measured to T1 = 160 ± 11 s and T2 ≈ 20 s. The resulting images of the flowing liquid were of reasonable quality and had an SNR of about 70.

Conclusion: Based on the SNR of the obtained Xe EPI images, it was estimated that rapid *in vivo* MRA with ^{129}Xe may be feasible, provided that an efficient, biologically acceptable carrier for Xe can be found and polarization levels of more than 25% can be achieved in isotopically enriched ^{129}Xe.

Key words: MR angiography, hyperpolarized gas; dissolved xenon-129; echo-planar imaging; experimental.

Correspondence: Sven Månsson, Department of Experimental Research, Malmö University Hospital, SE-205 02 Malmö, Sweden.
FAX +46 40 33 62 07.

Accepted for publication 10 June 2002.

In conventional proton MR imaging, only about 1 ppm of the available nuclei contribute to the observable NMR signal at thermal equilibrium and at clinical magnetic field strengths. However, by using optical pumping methods (5), it is possible to create non-equilibrium polarizations of noble gases (^{3}He and ^{129}Xe) 5–6 orders of magnitude higher than their thermal equilibrium polarization. MR imaging of hyperpolarized gases is thus possible, despite the low spin density (2, 17).

Imaging of hyperpolarized nuclei differs in several respects from traditional proton imaging. Once the hyperpolarized state is created, the longitudinal magnetization will decay towards the thermal equilibrium value with the time constant 1/T1. Typical imaging strategies for utilizing the initial magnetization are therefore to use gradient echo sequences with small radio frequency (RF) flip angles, or sequences which acquire the full *k*-space data after a single RF excitation, such as echo-planar imaging (EPI) (19), rapid acquisition with relaxation enhancement (RARE) (7) or spiral imaging (22). When imaging a low-gamma nucleus like xenon (Xe), attention must be paid to the per-

formance of the gradient system, since the time integral of the imaging gradients must be increased compared to proton imaging.

Although visualization of the respiratory airways and the lungs has been the primary target for the potential clinical use of hyperpolarized gases (13, 15), attempts have been made to assess the usefulness of hyperpolarized gases for other applications. With respect to vascular studies, Xe is soluble in biological tissues and, when inhaled, is taken up into the pulmonary blood. Applications such as functional MR imaging (fMRI) (9) and measurement of cerebral blood flow (20) have been suggested using inhaled hyperpolarized Xe. Various carriers have also been proposed as delivery media for Xe after i.v. injections (6, 21, 24). Injection of such solutions or emulsions of hyperpolarized Xe may be used for fMRI (10), perfusion measurements (6, 14) or MR angiography (MRA) (4).

MRA using hyperpolarized contrast media has the advantage of absence of background signal from surrounding tissues. The lack of background signal improves the contrast-to-noise ratio and may enable reduced field of view without folding artifacts, thereby allowing reduced matrix sizes and correspondingly faster acquisition times. Angiographic imaging using injected hyperpolarized ^{129}Xe has previously been reported (18). This study employed a gradient echo sequence with moderate flip angle and a few seconds' scan time. However, a fast single-shot acquisition technique, like EPI, could potentially improve the result, due to the full utilization of the longitudinal magnetization of the hyperpolarized contrast agent. Ultrafast imaging could furthermore reduce flow and motion artifacts, thereby opening possibilities for imaging of rapidly moving vessels, where conventional proton-based techniques are hampered by object motion and tissue background signal.

The use of hyperpolarized contrast agents for rapid MRA has to date been sparsely investigated and the feasibility of the technique needs further evaluation. It was the aim of the present study to evaluate the potential application of ^{129}Xe as an angiographical contrast agent, using EPI of a flow phantom. From the obtained signal-to-noise ratio (SNR) the efficacy of the EPI sequence was evaluated and predictions and extrapolations to clinical whole-body imaging were performed.

Material and Methods

Xe polarization and handling: ^{129}Xe was polarized with laser optical pumping using a prototype commercial polarizer (IGI 9800, Amersham Health, Durham, NC, USA). A gas mixture of 1% enriched Xe (75% ^{129}Xe), 10% N_2 and 89% ^{4}He flowed at a rate of 1.0 l/min through an optical cell where the ^{129}Xe spins were polarized via spin exchange with optically pumped Rb vapor (5). Hyperpolarized Xe (HpXe) was accumulated for 37 min and frozen at liquid nitrogen temperature. After thawing, the HpXe was collected in a plastic bag (volume 300 ml, Tedlar, Jensen Inert, Coral Springs, FL, USA) at 1 atm pressure. The polarization level in the bag immediately after thawing was measured to 6% using a stand-alone calibration station (Amersham Health). The HpXe bag was transported 40 m from the polarizer to the MR scanner in a transport suitcase (Amersham Health) with a static magnetic field of 0.5 mT. The first HpXe image was acquired 1 h after the polarization measurement. After the last HpXe image, the polarization of the gas remaining in the bag was again measured at the calibration station and the T1 relaxation within the bag was calculated. Using this T1 value, the actual polarization level at each imaging time point could be interpolated.

Dissolving of Xe gas in ethanol: A 60-ml plastic syringe (Plastipak; Becton Dickinson, Drogheda, Ireland) containing 25 ml 95% ethanol was connected to the HpXe bag. The syringe was filled with Xe gas from the bag to a total volume of 60 ml and intensely shaken for 3 s to achieve an equilibrium solution. Thereafter the remaining gas was removed from the syringe. To determine the amount of shaking necessary to reach an equilibrium solution, the concentration of dissolved HpXe was measured after intense shaking of the gas-ethanol mixture, after gentle shaking and without shaking. For determination of the concentration of dissolved HpXe, a syringe containing 50% ethanol volume and 50% HpXe gas volume after shaking was placed in the magnet and NMR spectra were acquired. The dissolved concentration was calculated from the ratio of the areas of the gas peak and the dissolved peak (163 ppm apart) and the known gas concentration at 1 atm pressure.

The T1 and T2 relaxation times of dissolved HpXe were measured in syringes containing only liquid (no gaseous HpXe). T1 relaxation was measured using a train of 16 RF excitations with 12 s interdelay time and a flip angle of 3°. Due to the small flip angle, the apparent relaxation caused by the RF pulses was ignored. The T1 relaxation was measured both with and without removal of solved oxygen from the ethanol, by intense bubbling with helium gas for 5 min, before mixing with HpXe. T2 relaxation was estimated using a Carr-Purcell-Meiboom-Gill (CPMG) multiecho sequence with

128 echoes and an interecho time of 100 ms. The T1 and T2 relaxation times were calculated by fitting of mono-exponential functions to the peaks of the dissolved HpXe spectral line. T2 relaxation was measured without He bubbling.

Flow phantom: A flow phantom was constructed consisting of two thin-walled (0.1 mm) plastic tubes with 6.0-mm inner diameter, inserted into a Plexiglas cylinder with 65-mm diameter (Fig. 1). The Plexiglas cylinder was filled with tap water in order to minimize susceptibility gradients from air-fluid boundaries. The plastic tubes were connected via flexible silicone tubing (5-mm inner diameter) to two glass containers, allowing free, gravity-induced flow of ethanol from the upper to the lower container through the phantom. The phantom was placed horizontally in the magnet. The vertical distance between the two containers was adjusted to give a mean flow velocity of 15 cm/s. The mean velocity was calculated from the measured flow (as measured by stop-watch and measure glass) divided by the cross-section area of the tube.

A 25-ml bolus of hyperpolarized Xe dissolved in ethanol was injected in the flow phantom through a plastic catheter 45 cm upstream from the magnet isocenter. The injection rate was approximately 12 ml/s. To ensure an even mixing of the injection bolus throughout the full diameter of the tube, the catheter was directed upstream relative to the flow direction. Image acquisition was started before the bolus injection and continued for 1 min.

MR imaging and image evaluation: Imaging was performed on a 2.4 T animal imaging system (Biospec 24/30, Bruker Biospin, Ettlingen, Germany) with a maximum gradient strength of 200 mT/m and a gradient rise time of 240 µs. The RF coil was a birdcage resonator double-tuned for ^{1}H and ^{129}Xe (Bruker Biospin). Flow phantom images of HpXe were acquired approximately 20 s after the mixing of HpXe with ethanol, using a single-shot, spin-echo EPI sequence. The readout gradient direction was aligned parallel to the flow direction (Fig. 1). The sequence parameters were: FOV 10×10 cm, matrix 32×32, echo time 32 ms, ADC bandwidth 50 kHz, total scan time 44 ms. The images were acquired without slice-selection gradients. During the bolus passage, images were acquired repeatedly with 1.5 s intervals.

For comparison, imaging was also performed using non-hyperpolarized Xe. A syringe filled with thermally polarized Xe dissolved in ethanol was placed in the magnet and a spin-echo EPI image was acquired with parameters: FOV 24×24 cm, matrix 64×64, echo time 192 ms, ADC bandwidth 25 kHz, without slice gradient. Due to the weak signal from the non-hyperpolarized Xe, the sequence was averaged 64 times with a repetition time of 300 s and a 90° flip-back pulse between each single-shot acquisition.

The time-course of the signal intensities in the flow phantom images was measured as the average signal within a central 1×5 pixel region perpendicular to the inflow and outflow tubes. The SNR of all images was measured as the mean signal within a region of interest (ROI) divided by the noise level σ. σ was estimated using the relation (11)

$$\sigma = \sqrt{\frac{2}{\pi}}\, S_{back} \qquad \text{(Eqn. 1)}$$

where S_{back} is the mean signal within a ROI containing only background noise. For the image of thermal equilibrium Xe, the measured SNR was corrected by the method suggested by Gudbjartsson & Patz (11) for low SNR images:

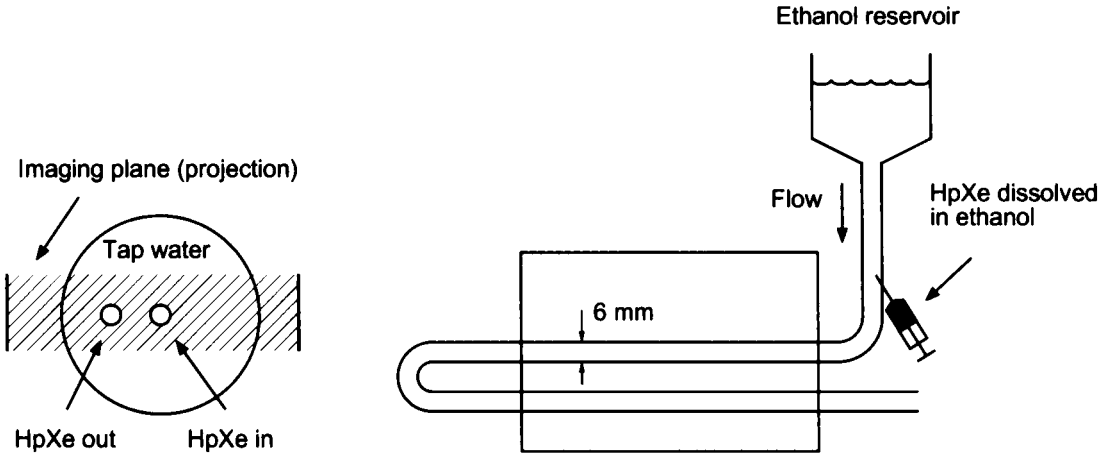

Fig. 1. The flow phantom and image orientation of the echo planar images. In the experiment, no slice selection gradient was used.

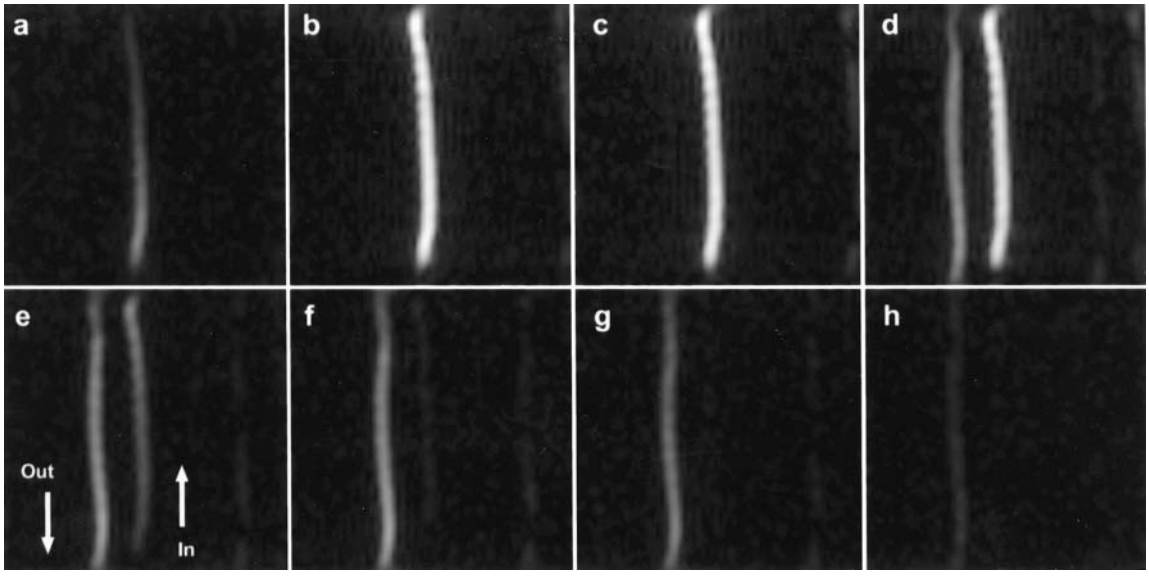

Fig. 2. a–h) EPI images showing a time series of flowing Hp ^{129}Xe, acquired at 1.5-s intervals. The acquisition time of each image was 44 ms. The flow direction is indicated in (e). The mean flow velocity was 15 cm/s and the HpXe polarization level was estimated to 2%.

$$S_{corrected} = \sqrt{|S^2 - \sigma^2|} \qquad \text{(Eqn. 2)}$$

where S is the measured signal intensity. Without this correction, the SNR of a noisy image would be overestimated.

To be able to compare the different SNR values, a normalization was made using the following relation (8):

$$SNR \propto cPV_{vox}\sqrt{t_{aq}} \qquad \text{(Eqn. 3)}$$

where c is the spin concentration, P is the polarization, V_{vox} is the voxel volume and t_{aq} is the total sampling time. The SNR was normalized to c=1 M, 10 mm^3 voxel volume, 1 s sampling time and P corresponding to thermal equilibrium polarization.

Results

Solution and relaxation properties: After intense shaking for 3 s, the measured Ostwald solubility coefficient (the ratio between dissolved concentration and gas concentration) of Xe in ethanol was 2.8±0.3, corresponding to 87±8 mM ^{129}Xe. Prolonged shaking (10 s) of the gas-ethanol solution did not significantly increase the solubility. With only gentle shaking, or without shaking, the solubility was 1.6±0.3, indicating that an equilibrium solution had not been reached.

The T1 relaxation of HpXe dissolved in ethanol was measured to 55±10 s without He bubbling, and to 160±11 s after He bubbling. The T2 relaxation was measured to 25 s.

Flow phantom images: A series of eight consecutive EPI images with 1.5-s intervals are presented in Fig. 2. The polarization level at the time of imaging was estimated to 2% when considering the T1 relaxations in both the Tedlar bag and the ethanol. The time course of the signal intensities are plotted for the inflow and the outflow tubes (Fig. 3). The delay between the arrival of the inflow and outflow boluses, as defined by the half-maximum intensity in the center of the image, was measured to 3.2 s. The dis-

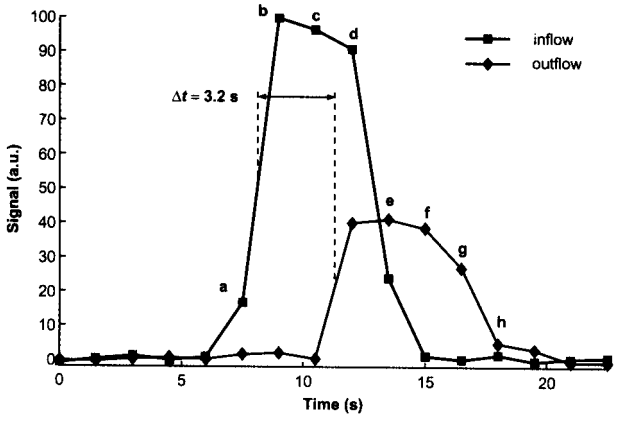

Fig. 3. Time course of the signal intensities in the EPI images of flowing hyperpolarized Xe. The time delay (Δt) of 3.2 s between the arrival of the inflow and outflow boluses corresponds to a mean flow velocity of about 17 cm/s. The letters a–h correspond to the images shown in Fig. 2.

tance traveled by the bolus was about 55 cm, hence the time delay corresponded to a mean flow velocity of 17 cm/s, which was in good agreement with the stop-watch measured flow of 15 cm/s.

The maximum SNR in the flow phantom images was measured to 74. The SNR of the thermally polarized Xe was 3.8 (after correction according to (11)). The normalized SNR values, according to Eqn. 3, were 14 (flow phantom) and 19 (thermal polarization), respectively.

Discussion

In the EPI images of the flowing, hyperpolarized Xe, no severe artifacts related to improper adjustment of the imaging gradients were visible, except a minor ghost in the phase encoding direction ("N/2-ghost"). The slight curvatures of the straight tubes in the flow phantom were caused by B_0-field inhomogeneities. The maximum SNR was measured to 74, and the images were of reasonable quality. The relatively coarse spatial resolution in the experiment (3 mm) was mainly dictated by the performance of the gradient system. From an SNR point of view, an increased spatial resolution would have been possible. The low polarization level during the experiment also leaves room for SNR improvements. When using Xe at thermal equilibrium, an EPI image could only be acquired after extensive averaging. After normalization according to Eqn. 3, the SNR of the hyperpolarized, flowing Xe was about 25% lower than the SNR of the thermal equilibrium, static Xe. A possible explanation for this difference could be flow-induced signal losses, but the normalized SNR values of the hyperpolarized and the non-hyperpolarized images were within the same range and thus indicated that no major, unexpected signal loss had taken place, e.g., during the process of solving the hyperpolarized gas in the ethanol. Neither did the experiments where the Ostwald solubility coefficient of HpXe in ethanol was investigated indicate any such polarization losses.

The Ostwald solubility coefficient of Xe in ethanol, as measured via the NMR procedure in the present study, agreed reasonably well with reported measurements of Ostwald solubility coefficients using radiographic methods (12), where the solubility was 2.47 ± 0.02. The measured T1 and T2 relaxation times of hyperpolarized Xe in ethanol are 1–2 orders of magnitude longer than the proton relaxation times within the body. Long relaxation times are essential for preserving the magnetization from the injection site to the target organ, but also for permitting fast, single-shot techniques, like the EPI sequence. Without a suitable carrier agent, the relaxation times of Xe in blood is short (T1 of 3–10 s depending on the oxygenation level (1), T2 of 2–7 ms) (23). When using lipid emulsion as a carrier, however, the relaxation times may be prolonged (T1 of 25 s, T2* of 37 ms) (18).

Taking the normalized SNR from the EPI images of flowing HpXe as a starting point, the SNR can be predicted for various scenarios. In our experiments, the polarization level during imaging was approximately 2%. With further developments of the optical pumping techniques, and by minimizing the delay between the dispensing of hyperpolarized gas and injection of HpXe, polarization levels of at least 25% can be expected for the injection solution (5). The concentration of HpXe after i.v. injection is more difficult to estimate because the bolus will be diluted by the ratio between the cardiac output and the injection rate (16). Furthermore, when passing the heart, a mixing of the Xe carrier with blood will occur, which has both a shorter T1 (3) and a lower solubility for Xe than the carrier. As a first approximation, one may consider the case of injecting a bolus with 25% polarization of enriched ^{129}Xe, and ignore relaxation and dilution of the bolus after injection.

The Ostwald solubility coefficient of Xe in, for example, perfluorcarbons is 1.2 (24), i.e., half of the solubility in ethanol. The bolus concentration would therefore be about 40 mM. Assuming the bolus being imaged with a scanner capable of gradient strengths of about 40 mT/m, it should be possible to acquire 64×64 matrix EPI images with $2 \times 2\,mm^2$ in-plane resolution within 70–80 ms. Based on the measured SNR from our experiments, we estimate that the SNR of such an image would result in usable angiograms (SNR about 20). This estimation is based on the assumptions that: a) Xe can be polarized to levels of at least 25%; b) isotopically enriched ^{129}Xe is used; c) the vessel diameters are >2 mm; and d) the Xe is solved in a carrier with a solubility of 1.2 or better. Admittedly, bolus dilution and polarization loss due to T1 relaxation after injection will diminish SNR and thus call for further increased polarization levels, and/or decreased spatial and temporal image resolution. Clearly, the usefulness of HpXe and the single-shot EPI technique as demonstrated in this work, will depend on whether biocompatible carriers with long relaxation times are available.

Conclusions: Using EPI acquisition, our experiments demonstrated that HpXe MRA images with 32×32 matrix could be acquired with $3 \times 3\,mm^2$ in-plane resolution in less than 50 ms. Despite the modest polarization level ($<3\%$) used in the present study, the image SNR was high (>70). Al-

though several technical issues remain to be improved, the experiments hold promise for the future use of HpXe as an MRA contrast agent in combination with ultrafast imaging for studies of, e.g., vessels subjected to internal motion.

REFERENCES

1. Albert M. S., Balamore D., Kacher D. F., Venkatesh A. K. & Jolesz F. A.: Hyperpolarized ^{129}Xe T1 in oxygenated and deoxygenated blood. NMR Biomed. 13 (2000), 407.
2. Albert M. S., Cates G. D., Driehuys B. et al.: Biological magnetic resonance imaging using laser-polarized ^{129}Xe. Nature 370 (1994), 199.
3. Albert M. S., Schepkin V. D. & Budinger T. F.: Measurement of ^{129}Xe T1 in blood to explore the feasibility of hyperpolarized ^{129}Xe MRI. J. Comput. Assist. Tomogr. 19 (1995), 975.
4. Chawla M. S., Chen X. J., Cofer G. P. et al.: Hyperpolarized ^{3}He microspheres as a novel vascular signal source for MRI. Magn. Reson. Med. 43 (2000), 440.
5. Driehuys B., Cates G. D., Miron E., Sauer K., Walter D. K. & Happer W.: High-volume production of laser-polarized ^{129}Xe. Appl. Phys. Lett. 69 (1996), 1668.
6. Duhamel G., Choquet P., Leviel J. L. et al.: *In vivo* ^{129}Xe NMR in rat brain during intra-arterial injection of hyperpolarized ^{129}Xe dissolved in a lipid emulsion. C. R. Acad. Sci. III 323 (2000), 529.
7. Durand E., Guillot G., Darrasse L. et al.: CPMG measurements and ultrafast imaging in human lungs with hyperpolarized helium-3 at low field (0.1 T). Magn. Reson. Med. 47 (2002), 75.
8. Edelstein W. A., Glover G. H., Hardy C. J. & Redington R. W.: The intrinsic signal-to-noise ratio in NMR imaging. Magn. Reson. Med. 3 (1986), 604.
9. Gao J. H., Lemen L., Xiong J., Patyal B. & Fox P. T.: Magnetization and diffusion effects in NMR imaging of hyperpolarized substances. Magn. Reson. Med. 37 (1997), 153.
10. Goodson B. M., Song Y., Taylor R. E. et al.: *In vivo* NMR and MRI using injection delivery of laser-polarized xenon. Proc. Natl. Acad. Sci. USA 94 (1997), 14725.
11. Gudbjartsson H. & Patz S.: The Rician distribution of noisy MRI data. Magn. Reson. Med. 34 (1995), 910.
12. Himm J. F.: The solubility of xenon in simple organic solvents and in aqueous amino acid solutions. Thesis, Michigan State University 1986.
13. Kauczor H. U., Hofmann D., Kreitner K. F. et al.: Normal and abnormal pulmonary ventilation. Visualization at hyperpolarized He-3 MR imaging. Radiology 201 (1996), 564.
14. Lavini C., Payne G. S., Leach M. O. & Bifone A.: Intravenous delivery of hyperpolarized ^{129}Xe. A compartmental model. NMR Biomed. 13 (2000), 238.
15. Macfall J. R., Charles H. C., Black R. D. et al.: Human lung air spaces. Potential for MR imaging with hyperpolarized He-3. Radiology 200 (1996), 553.
16. Maki J. H., Chenevert T. L. & Prince M. R.: Three-dimensional contrast-enhanced MR angiography. Top. Magn. Reson. Imaging 8 (1996), 322.
17. Middleton H., Black R. D., Saam B. et al.: MR imaging with hyperpolarized ^{3}He gas. Magn. Reson. Med. 33 (1995), 271.
18. Möller H. E., Chawla M. S., Chen X. J. et al.: Magnetic resonance angiography with hyperpolarized ^{129}Xe dissolved in a lipid emulsion. Magn. Reson. Med. 41 (1999), 1058.
19. Saam B., Yablonskiy D. A., Gierada D. S. & Conradi M. S.: Rapid imaging of hyperpolarized gas using EPI. Magn. Reson. Med. 42 (1999), 507.
20. Swanson S. D., Rosen M. S., Agranoff B. W., Coulter K. P., Welsh R. C. & Chupp T. E.: Brain MRI with laser-polarized ^{129}Xe. Magn. Reson. Med. 38 (1997), 695.
21. Venkatesh A. K., Zhao L., Balamore D., Jolesz F. A. & Albert M. S.: Evaluation of carrier agents for hyperpolarized xenon MRI. NMR Biomed. 13 (2000), 245.
22. Viallon M., Berthezene Y., Callot V. et al.: Dynamic imaging of hyperpolarized ^{3}He distribution in rat lungs using interleaved-spiral scans. NMR Biomed. 13 (2000), 207.
23. Wilson G. J., Santyr G. E., Anderson M. E. & Deluca P. M. Jr: T2 of ^{129}Xe in rat tissue homogenates and blood at 9.4 T. Proc. Ann. Meeting ISMRM 1999, p. 2102.
24. Wolber J., Rowland I. J., Leach M. O. & Bifone A.: Perfluorocarbon emulsions as intravenous delivery media for hyperpolarized xenon. Magn. Reson. Med. 41 (1999), 442.